The Journal of Chemical Physics

RESEARCH ARTICLE | JULY 24 2024

Accuracy limit of non-polarizable four-point water models: TIP4P/2005 vs OPC. Should water models reproduce the experimental dielectric constant?

L. F. Sedano ; S. Blazquez ; C. Vega

J. Chem. Phys. 161, 044505 (2024)
https://doi.org/10.1063/5.0211871

AIP Publishing

The Journal of Chemical Physics ARTICLE pubs.aip.org/aip/jcp

Accuracy limit of non-polarizable four-point water models: TIP4P/2005 vs OPC. Should water models reproduce the experimental dielectric constant?

Cite as: J. Chem. Phys. 161, 044505 (2024); doi: 10.1063/5.0211871
Submitted: 2 April 2024 • Accepted: 30 June 2024 •
Published Online: 24 July 2024

L. F. Sedano, S. Blazquez, and C. Vega[a)]

AFFILIATIONS

Departamento de Química Física, Facultad de Ciencias Químicas, Universidad Complutense de Madrid, 28040 Madrid, Spain

[a)]Author to whom correspondence should be addressed: cvega@quim.ucm.es

ABSTRACT

The last generation of four center non-polarizable models of water can be divided into two groups: those reproducing the dielectric constant of water, as OPC, and those significantly underestimating its value, as TIP4P/2005. To evaluate the global performance of OPC and TIP4P/2005, we shall follow the test proposed by Vega and Abascal in 2011 evaluating about 40 properties to fairly address this comparison. The liquid–vapor and liquid–solid equilibria are computed, as well as the heat capacities, isothermal compressibilities, surface tensions, densities of different ice polymorphs, the density maximum, equations of state at high pressures, and transport properties. General aspects of the phase diagram are considered by comparing the ratios of different temperatures (namely, the temperature of maximum density, the melting temperature of hexagonal ice, and the critical temperature). The final scores are 7.2 for TIP4P/2005 and 6.3 for OPC. The results of this work strongly suggest that we have reached the limit of what can be achieved with non-polarizable models of water and that the attempt to reproduce the experimental dielectric constant deteriorates the global performance of the water force field. The reason is that the dielectric constant depends on two surfaces (potential energy and dipole moment surfaces), whereas in the absence of an electric field, all properties can be determined simply from just one surface (the potential energy surface). The consequences of the choice of the water model in the modeling of electrolytes in water are also discussed.

I. INTRODUCTION

Water's unique physical and chemical properties make it indispensable for life as we know it, playing a central role in biology, meteorology, energy resources, etc.[1] Its peculiar behavior as compared to other substances has been widely studied.[2–4] The first and well-known density anomaly was reported in 1805 by Hope.[5] Water presents a maximum in density at 4 °C, which results in the solid phase (ice Ih) at ambient conditions being less dense than the liquid. Furthermore, these anomalies are strengthened in the metastable supercooled regime.[6] For these reasons, computer simulations have played a key role in trying to improve our understanding of the behavior of this complex molecule. A good force field describing the interaction between the molecules is paramount for simulations to avoid spurious effects. Ideally, the interaction energy of a certain configuration should be obtained from quantum chemistry calculations.[7] However, almost exact quantum calculations can be performed only for small clusters, and faster Density Functional Theory (DFT) calculations[8,9] are merely approximations. In addition, these calculations are still computationally expensive and unattainable for investigating certain topics. For instance, biological systems,[10,11] nucleation events,[12–14] or water under extreme conditions[15–17] require a simpler and faster (although admittedly less accurate) description of the interaction energy of the system to be computationally feasible. The simplest way to perform atomistic simulations is to employ a rigid non-polarizable force field.

The history of these water models in computer simulations is long. They are often classified by the number of interaction centers, three (3C), four (4C), and five (5C). Non-polarizable water

models have typically only one Lennard-Jones (LJ) center located at the position of the oxygen and rigid bond distances (introducing flexibility does not significantly improve their performance[18]). Since one of the main aims of this work is to analyze whether we have already reached the limit of what can be done using non-polarizable models, it seems pertinent to provide a brief historical perspective of the work done in the last fifty years (see also Ref. 19 for another historical description). We will divide it into seven different periods. Although this is certainly arbitrary, we do hope it may help to understand the evolution of the field.

1933. Bernal and Fowler[20] proposed the first model of water. Two positive partial charges were located at the hydrogen atoms, and a negative one was positioned along the H–O–H bisector. A Lennard-Jones center was placed at the oxygen.

1970–1980. During this decade, the pioneering studies of Barker–Watts[21] and Rahman and Stillinger[22] took place. The goal was to show that simulations of water were indeed feasible. The potential model that emerged from this period was ST2,[23] which is a 5C model with positive partial charges on the hydrogens and negative charges on the lone pair electrons.

1980–1986. Two experimental properties were used to tune the potential parameters, namely, the density of water and the vaporization enthalpy (ΔH_v) at room temperature. That brought a new wave of water models specially designed to reproduce these two properties as, for instance, the SPC[24] (3C), the TIP3P (3C),[25] and the TIP4P (4C).[25] For the SPC and the TIP3P, the negative charge is located at the oxygen atom, whereas for TIP4P, it is positioned along the bisector of the H–O–H angle, as in the first water model from 1933.[20]

1987. Berendsen and co-workers proposed the SPC/E model of water[26] (3C) introducing a somewhat revolutionary idea: the so-called "self-polarization energy," which accounts for differences in the internal energy due to the electronic redistribution of water in different phases. The statement was made that rigid non-polarizable models should only reproduce ΔH_v after this correction was included. Classical simulations of non-polarizable models are expected to yield vaporization enthalpies that exceed experimental values. First, this is attributed to nuclear quantum effects, which reduce vaporization enthalpy by ~0.4 kcal mol^{-1}, evident when comparing the vaporization enthalpies of T_2O and H_2O.[27,28] Second, the electronic redistribution of water molecules in the condensed phases (polarization) cannot be implemented in classical simulations. These facts defy the idea that the vaporization enthalpy should be used as a target property when developing water force fields. Furthermore, in 2011, Vega and Abascal conducted an extensive evaluation of rigid non-polarizable models (hereinafter referred to as VA-Test).[29] In this assessment, the SPC/E model scored 5.1 out of 10, surpassing the TIP3P (2.7) and the TIP4P (4.7), thereby confirming the superiority of Berendsen's approach.

2000. A new 5C water model TIP5P was presented by Mahoney and Jorgensen[30] introducing a new idea, namely, to use the temperature of the maximum in density (TMD) of water along the room pressure isobar as a target property. That was indeed a bright idea, hitherto never considered (although admittedly the estimation of this property required very long runs, which were not feasible before that date). However, Berendsen's suggestion was not adopted since the model was forced to reproduce the experimental value of the vaporization enthalpy. It was later shown that the melting point for this model was quite good, and so was the difference between the melting temperature and the TMD (11 K, close to the experimental difference of 4 K), which is much smaller than the 25 K difference observed for most 3C and 4C models[31] (and even for some polarizable ones[32]). Further research showed that it failed in predicting the vapor–liquid equilibria, surface tension, and response functions (i.e., the isothermal compressibility, thermal expansion coefficient, and the heat capacity).[29] In addition, its phase diagram is flawed, mainly due to the fact that the lone pair electron overestimates the tetrahedrality of ices, leading to too high densities for ice polymorphs and the over-stabilization of ice II.[33,34] The score of the TIP5P in the VA-Test was 3.7, lower than that obtained by SPC/E, tempering the initial excitement awaken by this model.

2004–2005. A new wave of rigid and non-polarizable water models emerged combining the ideas proposed by the groups of Berendsen *et al.*[26] and Mahoney and Jorgensen,[30] that is, respectively, to include the self-polarization energy term by purposely overestimating the enthalpy of vaporization and establishing the TMD as a key target property. The adopted geometry was that of the TIP4P, after it had been shown that 3C models tended to provide poor predictions of the phase diagram of water due to an incorrect interplay between the forces of the dipole and the quadrupole moment[31,35] and too low values for both the melting temperature of ice and the temperature of the density maximum.[36] Finally, a technical but relevant issue was addressed: Coulombic interactions were not simply truncated at the cutoff distance as previously done, but Ewald sums[37] were incorporated to the simulations to properly deal with the charges. It was at that time that the TIP4P-Ew[38] and the TIP4P/2005[39] models were proposed. The main difference between these two models lies in the distance between the oxygen atom and the location of the negative charge at the M center. According to the VA-Test, the performance of the TIP4P/2005 model scored 7.2, significantly improving the description of water compared to all its predecessors.[29] However, these two models failed in reproducing the dielectric constant of water ε_r as they underestimated it (by approximately a 25% compared to the experimental value). Some models proposed after 2005, still followed the overall spirit of that time (TIP4P geometry, reproducing the TMD, overestimating ΔH_v, and having low values of ε_r) and can be ascribed to this family of potentials, as, for instance, TIP4P-D[40] and a recently developed model by Jungwirth and co-workers: ECCw2024.[41] For reasons that will be discussed below, these water force fields will be denoted as ECC models.

2014–2018. After noticing that the dielectric constant for liquid water of TIP4P-Ew and TIP4P/2005 was too low when compared to the experimental values, several groups initiated the search of a model with a better dielectric constant. The TIP4P geometry was adopted, given its proven success, although allowing for deviations of the experimental bond lengths and angles, which adds extra degrees of freedom to the fit. The key ideas of the 2000–2005 period were preserved: Ewald sums were applied to deal with the Coulombic interactions, the TMD was used for fitting the parameters, and the enthalpy of vaporization was disregarded. However, and this is the main difference with the models of the 2004–2005 period, the dielectric constant of water was included as a target property. The models proposed at that time were TIP4P/ε,[42] TIP4P-FB,[43] and OPC,[44] which are similar in spirit. We shall denote these models as non-ECC models, as opposed to the ones from the previous period.

Let us now describe the origin of the ECC or non-ECC notation. Leontyev and Stuchebrukhov in a series of papers[45–47] pointed out that non-polarizable models do not mimic the fast response of electrons to an external electric field. The dielectric constant of liquid water at high frequencies (ε_∞) tends to a value of about 1.75. Taking into account that the dielectric constant is proportional to μ^2 [see Eq. (1)], the electronic polarization should increase the dipole moment of water by $\sqrt{1.75}$ = 1.32. Non-polarizable force fields do not incorporate this contribution, and therefore, their dipole moments yield smaller values (≈2.2–2.3 D) than the expected value in liquid water (≈2.8–3.0 D).[48–52] The mean field approximation accounting for this lack of polarizability is known as the Electronic Continuum Correction (ECC). Thus, non-ECC models are those that neglect the electronic continuum corrections by purposely targeting the dielectric constant of water, as opposed to ECC models. Therefore, we arrive at the conclusion that fitting the dielectric constant is not a matter of merely adding another parameter to the fitting procedure, but rather constitutes a conceptual quandary. Vega showed that ε_r differs from other properties because of its dependence not only on the Potential Energy Surface (PES) but also on the Dipole Moment Surface (DMS).[53] He claimed, putting forward theoretical arguments that the partial charges used to describe both surfaces need not be the same since the PES and DMS are independent. In addition, the point charges used in non-polarizable models are approximations and lack any physical meaning, therefore discarding the possibility of a "correct" election of the charges. Obviously, the position and magnitude of the charges determine the dipolar moment. Thus, dipole moments providing a good description of the PES of water (around 2.3 D) are significantly smaller than those needed to describe the DMS (around 2.9 D[48–52,54,55]), and the same can be said for other substances as well.[56,57]

For a non-polarizable force field, the expression of the dielectric constant (under Ewald conducting boundary conditions[37,58,59]) is as follows:

$$\varepsilon_r = 1 + \frac{4\pi\rho\mu^2 G}{3k_B T}, \tag{1}$$

where ρ is the number density, k_B is the Boltzmann constant, T is the temperature, μ is the dipole moment of the molecule of water in the non-polarizable model of water, and G is the polarization factor that measures the orientational fluctuations of the unit vectors of the dipoles. Equation (1) is paramount for understanding the differences between ECC and non-ECC models. The dipole moment μ of the ECC non-polarizable force field is much smaller (by about 20%–30%) than the true dipole moment of water in the liquid phase, and therefore, the dielectric constant is expected to be severely underestimated when using this formula despite a correct description of G.[54] Although non-ECC models tend to have larger dipole moments (2.4–2.49 D),[42–44] their values are still lower than the expected true dipole moment of water in the condensed phase (≈2.9 D[48–52]). From Eq. (1), it is evident that since μ is still underestimated by non-ECC models, its square should yield a dielectric constant lower than the experimental one if G was properly described.

After this historical introduction, we arrive at the question that motivated this work: Are non-ECC models of water superior to ECC models in describing the overall properties of water? To answer it, we shall implement the VA-Test using the properties and the score system proposed in the original paper.[29] We evaluate about 40 properties (grouped in 14 categories). The resulting numerical outcome for each property is obtained from the relative error of the water model when compared to the experimental result as described in Ref. 29 and briefly summarized in Sec. III. We compare two representative models of the ECC and non-ECC categories: TIP4P/2005 and OPC, respectively. The TIP4P/2005 model is well established as a reliable choice for modeling water, accurately reproducing many of its properties and earning recognition as one of the best rigid and non-polarizable models.[17,29,33,60–64] The OPC is selected as a workcase of the non-ECC family. In fact, the manual of AMBER[65,66] states that OPC should be regarded as a suitable force field for replacing the widely (but far from satisfactory) TIP3P model. To implement the VA-Test, we have computed a number of properties for the OPC that have not been reported so far. It will be shown that OPC, despite being a good water potential, obtains a lower score than TIP4P/2005. It must be noted that although both models follow the key ideas for developing a well-behaved non-polarizable model (accounting for polarization energy, negative charge located on the H–O–H bisector, and using PME for the Coulombic potential), the target properties used to obtain the parameters for each water model were slightly different. TIP4P/2005 targeted the TMD, the density at 298 K, the density of ice (II) and ice (V), the enthalpy of vaporization at room temperature, and the stability of ice (III). OPC used as target properties the density, enthalpy of vaporization, diffusion coefficient, location and height of the first peak of the oxygen–oxygen radial distribution function, and the dielectric constant (all at room temperature and pressure). However, since TIP4P/2005 and OPC yield very similar radial distribution functions, TMDs, and self-diffusion coefficients (see Table II and the supplementary material), it is clear that the main difference in the design of both models is to include (OPC) or not (TIP4P/2005) the dielectric constant as a target property. Notice that this difference is also conceptual as it suggests that it is possible to reproduce both the PES and the DMS with the same set of charges (this is the key assumption in the development of OPC) or to admit that it is not possible to reproduce both surfaces with the same set of charges (this is a key assumption in the development of TIP4P/2005). Thus, it appears that reproducing the dielectric constant can be directly associated with the slight decline in the overall performance of the OPC water model. This very fact prompts the conclusion that we have reached the limit of non-polarizable models with the 4C geometry and that further improvement within this geometry although possible would be quite small. Recently, a comparable conclusion has been drawn regarding the 3C geometry,[67,68] although 4C models notably enhance the performance of 3C models. Finally, we would like to point out that the adoption[41,53–57,69–75] or rejection of the ECC approach holds significant implications in the study of electrolyte solutions, being the charge of the ions related to the dielectric constant through the Debye–Hückel (DH) theory,[76,77] as will be discussed at the end of Sec. III.

II. METHODOLOGY AND SIMULATION DETAILS

To implement the VA-Test, several properties need to be evaluated. For the TIP4P/2005, all properties were already reported

TABLE I. Force field parameters for TIP4P/2005 and OPC water models.

Model	Charge (e)	σ_{ii} (Å)	ϵ_{ii} (kJ/mol)	d_{OH} (Å)	d_{OM} (Å)	Θ (°)	μ (D)	Q_T (DÅ)
TIP4P/2005								
O	0	3.158 9	0.774 9	0.9572	0.1546	104.52	2.305	2.297
H	0.5564							
M	−1.1128							
OPC								
O	0	3.166 55	0.890 36	0.8724	0.1594	103.6	2.48	2.3
H	0.6791							
M	−1.3582							

in the original 2011 paper, and we will use the values from that publication.[29] However, some properties (marked in bold font in Table I) have been recalculated in this work for the TIP4P/2005 to improve the accuracy of the originally reported values. Nevertheless, for OPC, we have computed all the properties required for the VA-Test. The parameters of both models are summarized in Table I. For the liquid phase, we have performed *NpT* simulations at 1 bar using the GROMACS 4.6.7 package with systems of 555 water molecules for the TIP4P/2005 and the OPC potentials. All the simulations were run with double precision. The leap-frog algorithm was used with a time step of 2 fs for integrating the equations of motion, and the water geometry was constrained with the LINCS algorithm.[78] The pressure and temperature were fixed by using an isotropic Parrinello–Rahman barostat[79] and the Nose–Hoover thermostat[80] with 2 ps relaxation times. Energy and pressure corrections were included to the LJ part of the potential. The cutoff employed was 10 Å for both electrostatic and dispersive forces. Simulations were carried out with the particle mesh Ewald (PME) to deal with electrostatics.[81] We run 200 ns on average and discarded the equilibration time (10–20 ns) for estimating the densities and its derivative properties (heat capacity, isothermal compressibility, and thermal expansion coefficient). The heat capacity and the isothermal compressibility were estimated from these runs by the well-known expressions of the fluctuations in the enthalpy and the volume, respectively,

$$\kappa_T = \frac{\langle \Delta V^2 \rangle}{k_B T \langle V \rangle}, \qquad C_p = \frac{\langle \delta H^2 \rangle}{k_B T^2}, \tag{2}$$

where V stands for the volume of the system and H stands for its enthalpy. Liquid simulations comprised the range of temperatures between 240 and 450 K. The densities as a function of temperature were fitted to a third-order polynomial. It is worth mentioning that when fitting the simulation points, it is a good practice[82] to have the same distance in degrees on either side of the maximum since the density decays more rapidly at temperatures lower than the TMD. Fitting only the right-side part of the density curve has led to under-estimations of around 2 K for this property in the past.[42] Therefore, the temperatures comprised for determining the TMD were 245–300 K for OPC and 245–315 K for TIP4P/2005. The thermal expansion coefficient α_p was also calculated,

$$\alpha_p = \frac{1}{V}\left(\frac{\partial V}{\partial T}\right)_p = \rho\left(\frac{\partial (1/\rho)}{\partial T}\right)_p. \tag{3}$$

Since both models are non-polarizable and rigid, the dielectric constant is simply obtained by the following expression when conducting periodic conditions are applied:[37,58,59]

$$\varepsilon_r = 1 + \frac{4\pi}{3 k_B T V}\langle M_x^2 + M_y^2 + M_z^2 \rangle, \tag{4}$$

where M_x is the value of the component X of the total dipole moment. For the solid phases, all the simulation details remain the same, but an anisotropic Parrinello–Rahman barostat was used instead.[79,83] Simulations of 10–20 ns were enough for calculating the densities of different ice polymorphs.

Regarding the liquid–vapor properties, we performed *NVT* simulations of direct coexistence using GROMACS 2018 for 15 ns with a box comprised of 6660 molecules The size of the simulation box was $L_x = L_y = 5.23$ nm and $L_z = 16$ nm (being the z axis perpendicular to the liquid–gas interface). The leap-frog algorithm was used with a time step of 2 fs. The temperature was fixed with the Nosé–Hoover thermostat with a coupling of 2 ps. We used PME both for electrostatics and for the LJ part of the potential. The real space contribution was truncated at 14 Å. The Fourier space contribution was computed using a spacing of 0.15 nm. The tolerance was set at 0.001. Notice that since we are using PME, the potential is not truncated. From these simulations, we calculated the orthobaric coexisting densities of both phases through the density profile. This also enabled the estimation of the vapor pressure (p_v) at coexistence, which is merely the component of the pressure perpendicular to the interface (p_N). Finally, the surface tension σ was obtained by computing the components of the pressure tensor,[84]

$$\sigma = \frac{L_z}{2}[p_N - p_T] = \frac{L_z}{2}\langle P_{zz} - \frac{1}{2}(P_{xx} + P_{yy})\rangle. \tag{5}$$

The simulation points of the surface tension were fitted to the following expression:[85]

$$\sigma = c_1\left(1 - \frac{T}{T_c}\right)^{11/9}\left[1 - c_2\left(1 - \frac{T}{T_c}\right)\right], \tag{6}$$

where the first term represents the Guggenheim[86] corresponding-state law. The vapor pressure has been adjusted to Antoines' law,[87]

$$\ln(p_v) = A_{pv} + \frac{B_{pv}}{T + C_{pv}}. \quad (7)$$

The difference in density between the liquid ρ_l and the gas ρ_g phase at coexistence was fitted to the following expression:[63]

$$\rho_l - \rho_g = A_0|\tau|^{\beta_c} + A_1|\tau|^{\beta_c+\Delta} + A_2|\tau|^{\beta_c+2\Delta} + A_3|\tau|^{\beta_c+3\Delta}, \quad (8)$$

where $\tau = 1 - T/T_c$, $\beta_c = 0.325$, and $\Delta = 0.5$. Similarly, the sum of the liquid and gas densities can be written[63] as

$$\rho_l + \rho_g = 2\rho_c + D_{1-\alpha}|\tau|^{1-\alpha} + D_1|\tau|, \quad (9)$$

where we used the value $\alpha = 0.11$.

For computing the transport properties, a larger system was employed (4440 molecules). We first equilibrated the system for 20 ns in a *NpT* simulation. Subsequently, we simulated the system for 50 ns in the *NVT* ensemble, for which the pressure tensor, $P_{\alpha\beta}(t)$ (for components with $\alpha \neq \beta$), was saved on disk every 2 fs. The shear viscosity was evaluated using the methodology proposed by González and Abascal[88] following the Green–Kubo formalism,

$$\eta = \frac{V}{k_B T}\int_0^\infty \langle P_{\alpha\beta}(t)\, P_{\alpha\beta}(0)\rangle\, dt. \quad (10)$$

For the diffusion coefficients (D), we used the Einstein relation,

$$D = \lim_{t\to\infty} \frac{1}{6t}\left\langle [\mathbf{r}_i(t) - \mathbf{r}_i(0)]^2 \right\rangle, \quad (11)$$

where $\mathbf{r}_i(t)$ and $\mathbf{r}_i(0)$ are the position of the ith particle at time t and at a certain origin of time, respectively.

The melting point of ice Ih was determined by using the direct coexistence technique.[89,90] A solid phase containing 2000 molecules of ice Ih was put in contact with 2000 molecules of liquid water by exposing the secondary prismatic plane of ice. Once again, we utilized the Nosé–Hoover thermostat and an anisotropic Parrinello–Rahman barostat with a relaxation time of 2 ps. The cutoff radius was set at 10 Å for dispersive and electrostatic interactions. Long-range corrections to the pressure and the energy for the LJ part of the potential were applied, and PME was used for the Coulomb potential.

A final comment regarding theoretical corrections is necessary. All the results presented in this study comprise raw data obtained from simulations without any *ad hoc* adjustments, whether theoretically or conceptually appropriate.[19,26,46] Theoretical corrections can provide valuable insights into understanding the shortcomings of a model. Various corrections have been proposed for several properties, such as the vaporization enthalpy,[19,26] or for the heat capacity (attributable to nuclear quantum effects).[38] However, incorporating such corrections may erroneously suggest that the models accurately describe experimental properties when, in fact, they do not.

It is important to note that corrections for finite size effects, such as the Yeh–Hummer correction for diffusion coefficients,[91] belong to a distinct category. These corrections address issues arising from the utilization of small system sizes in the simulations. They should be regarded as adjustments to the simulations rather than to the model itself. Thus, the transport properties computed here were obtained for systems containing 4440 molecules, and for the diffusion coefficients, we included the Yeh–Hummer corrections.[91]

III. RESULTS

All the properties computed in this work for OPC and TIP4P/2005 are presented in Table II. For each property, a certain score S between zero (poor agreement with experiment) and ten

TABLE II. Calculated properties for the selected ECC (TIP4P/2005) and non-ECC (OPC) models. For the OPC, all the results shown here were obtained in this work. For TIP4P/2005, all the values were reported in 2011.[29] The recalculated values from this work for TIP4P/2005 are shown in bold. In italics, we show the targeted properties of each model. For the diffusion coefficients, we also provide the numerical value of the D in square brackets [D × 10^5].

	Exp.	TIP4P/2005	OPC
Enthalpy of phase change (kcal/mol)			
ΔH_{melt}	1.44	1.13	1.07
ΔH_{vap}	10.52	*11.99*	*12.90*
Critical properties			
T_c (K)	647.1	641.4	697
p_c (bar)	220.64	146	168
ρ_c (g cm^3)	0.322	0.31	0.291
Surface tension (mN m^{-1})			
σ_{300K}	71.7	69.3	75.3
σ_{450K}	42.88	41.8	54.3
Melting properties			
T_{melt} (K)	273.15	**250** 252	244.5
ρ_{liq} (g/cm^3)	0.997	0.994	0.996
ρ_{solid} (g/cm^3)	0.917	0.921	0.895
dp/dT (bar K^{-1})	−140	−132	−90
Orthobaric densities (g/cm^3) and TMD (K)			
TMD	277	*277.3*	270.1
ρ_{298K}	0.999	***0.997*** *0.993*	*0.998*
ρ_{400K}	0.9375	**0.935** 0.93	0.942
ρ_{450K}	0.8903	**0.885** 0.879	0.900
Isothermal compressibility (10^{-6}/bar^{-1})			
κ_T (1 bar; 298.15 K)	45.3	**46.4** 46	44.5
κ_T (1 bar; 360 K)	47	50.9	44.4
Gas properties			
p_v (bar) (350 K)	0.417	0.13	0.07
p_v (bar) (450 K)	9.32	4.46	2.45

TABLE II. (*Continued*.)

	Exp.	TIP4P/2005	OPC
Heat capacity at constant pressure (cal mol^{-1} K^{-1})			
C_p (liq 298.15 K; 1 bar)	18	**21.4** 21.1	20.20
C_p (ice 250 K; 1 bar)	8.3	14	15.50
Tm-TMD-Tc ratios			
Tm(Ih)/Tc	0.422	0.390	0.351
TMD/Tc	0.428	0.432	0.388
TMD-Tm	4	27	25.6
Static dielectric constant			
ϵ_r (liq; 298 K)	78.5	57	*78*
Densities of ice polymorphs (g cm^{-3})			
ρ (I_h 250 K; 1 bar)	0.92	**0.921** 0.921	0.894
ρ (II 123 K; 1 bar)	1.19	***1.211*** *1.199*	1.176
ρ (V 223 K; 5.3 kbar)	1.283	***1.272*** *1.273*	1.239
ρ (VI 225 K; 11 kbar)	1.373	**1.369** 1.38	1.335
EOS high pressure (g/cm^3)			
ρ (373 K; 10 kbar)	1.201	1.204	1.189
ρ (373 K; 20 kbar)	1.322	1.321	1.299
Self-diffusion coefficient (cm^2 s^{-1})			
ln(D_{278K}) [D ×10^5]	−11.24 [1.31]	−11.23 [1.33]	−11.14 [1.46]
ln(D_{298K}) [D ×10^5]	−10.68 [2.30]	−10.67 [2.32]	*−10.65 [2.38]*
ln(D_{318K}) [D ×10^5]	−10.24 [3.57]	−10.25 [3.52]	−10.25 [3.52]
E_a (kJ/mol)	18.4	18.0	16.3
Shear viscosity (mPa s)			
η (1 bar; 298 K)	0.90	0.82	0.79
η (1 bar; 373 K)	0.28	0.28	0.30

(good agreement with experiment) will be assigned following the expression proposed by Vega and Abascal,[29]

$$S = \max\left\{anint\left[10 - abs\left(\frac{(X - X_{\text{exp}})\cdot 100}{X_{\text{exp}}\cdot tol}\right)\right],\ 0\right\}, \qquad (12)$$

where X is the magnitude obtained by the water model under consideration, X_{exp} is the experimental value, and *anint* is the nearest integer Fortran function. This is equivalent to the function of worksheets denoted as round function. Notice that there was a typo in Eq. (1) of Ref. 29 where *min* (minimum) was written instead of *max* (maximum). The magnitude *tol* (tolerance) represents a percentage deviation, and it adopts the values 0.5, 2.5, and 5 per cent depending on the property. We shall mirror all the tolerance values selected in the original publication.[29] If the prediction is within 0.5 times, the tolerance the score is ten points. If the deviation is between the 1.5 and 0.5 times the tolerance, the score is nine points, and so on. For a

TABLE III. Scores for all the properties computed in this work for the ECC (TIP4P/2005) and non-ECC (OPC) models. The values in bold are the average score from each block of properties.

	TIP4P/2005	OPC
Enthalpy of phase change	**5.0**	**3.0**
ΔH_{melt}	6	5
ΔH_{vap}	4	1
Critical properties	**7.3**	**6.0**
T_c	10	7
p_c	3	5
ρ_c	9	6
Surface tension	**9.0**	**4.0**
σ_{300K}	9	8
σ_{450K}	9	0
Melting properties	**8.5**	**5.8**
T_{melt}	7	6
ρ_{liq}	9	9
ρ_{solid}	9	5
dp/dT	9	3
Orthobaric densities and TMD	**9.5**	**9.0**
TMD	10	9
ρ_{298K}	10	10
ρ_{400K}	9	9
ρ_{450K}	9	8
Isothermal compressibility	**9.0**	**9.5**
κ_T (1 bar; 298.15 K)	10	10
κ_T (1 bar; 360 K)	8	9
Gas properties	**0**	**0**
p_v (350 K)	0	0
p_v (450 K)	0	0
Heat capacity at constant pressure	**3.0**	**4.0**
C_p (liq 298.15 K; 1 bar)	6	8
C_p (ice 250 K; 1 bar)	0	0
Tm-TMD-Tc ratios	**7.7**	**7.0**
Tm(Ih)/Tc	8	7
TMD/Tc	10	8
TMD-Tm	5	6
Static dielectric constant	**5.0**	**10**
ϵ_r (liq; 298 K)	5	10
Densities of ice polymorphs	**8.3**	**4.8**
ρ (I_h 250 K; 1 bar)	10	4
ρ (II 123 K; 1 bar)	6	8
ρ (V 223 K; 5.3 kbar)	8	3
ρ (VI 225 K; 11 kbar)	9	4
EOS high pressure	**10**	**7.5**
ρ (373 K; 10 kbar)	10	8
ρ (373 K; 20 kbar)	10	7
Self-diffusion coefficient	**9.0**	**8.5**
ln(D_{278K})	9	9
ln(D_{298K})	9	9
ln(D_{318K})	8	8
E_a	10	8
Shear viscosity	**9.0**	**8.5**
η (1 bar; 298 K)	8	8
η (1 bar; 373 K)	10	9
Total score	**7.2**	**6.3**

deviation larger than ten times the tolerance, we assign zero points. The score S is obtained after evaluating the relative error of a certain property by the water force field. In this way, a value is assigned for each property, which is then encompassed into thematic blocks that are finally averaged with equal weights, obtaining a global score for each model. All the scores are collected in Table III.

We begin by presenting the liquid–vapor equilibria for the OPC model, which has not been studied extensively. The coexistence densities for both models are depicted in Fig. 1. The critical temperature (T_c) for the OPC has been calculated following Eqs. (6) and (8) for six temperatures between 500 and 625 K. Equation (6) was truncated in the second term (using only the parameters A_0, A_1, and τ for the non-linear fit). The estimates from both equations differ only by 1 K, leading to an average value of T_c = 697 K. The critical density is simply obtained by representing the semi-sum of the liquid and the vapor densities as shown in Eq. (9) and extrapolating it to T_c. It can be seen that the TIP4P/2005 model provides remarkable results for both phases, closely aligning with the experimental critical temperature and density. In contrast, the densities of the OPC model begin to deteriorate above 500 K, leading to a higher critical temperature (T_c) and a slightly lower critical density (ρ_c) than the experimental ones. The results for the critical properties are collected in Table II.

The surface tension (σ) remained an elusive property for molecular simulations at the beginning, yielding different values from various studies, since it is very susceptible to the system size[96] and to the truncation of the potential,[97] both which increase the computation time. Due to the unlike densities of both phases, when this property is calculated via direct-coexistence, tail corrections must be included, as shown by previous studies.[64,93,98–100] Nevertheless, with current computational resources, these problems can be overcome by using PME both for the electrostatics and for the LJ potential, as we do in this work (see Sec. II). In Fig. 2, σ is depicted as a function of temperature for the TIP4P/2005 (from Refs. 64 and 93) and for the OPC along with experimental results.[94,95] It can be seen that the TIP4P/2005 provides excellent results for the surface tension. On the contrary, the OPC model overestimates σ across the entire range of temperatures studied, exhibiting an approximate constant offset of 8 mJ/m^2. Our value at 300 K of σ for OPC is in good agreement with the value reported by Tempra *et al.*[101] at 298 K.

On the other hand, the results of the vapor pressure for both models as a function of temperature are summarized in Fig. 3. It is notable that neither model is able to reproduce this property, although the underestimation of the OPC is significantly larger than that of the TIP4P/2005. Despite this fact and due to the large overestimation of the critical temperature of the OPC, its critical pressure is closer to the experimental one if compared with the TIP4P/2005. Nevertheless, the deviation is still large (around 25%). The fact that most non-polarizable models fail to reproduce the vapor pressure was already pointed out by Vega and Abascal,[29] with the notable exception of TIP4P[102] (at the cost of deteriorating other properties).

Notice that p_v can only be estimated by direct coexistence for moderately high temperatures (ideally above 400 K), where the pressure is at least of a couple bars, so the magnitude is significantly higher than its error. Thus, the lowest temperature for which we have estimated the vapor pressure in this work is 450 K (a less precise value of p_v is found in Table II at 350 K, where the vapor pressure was estimated through the density profile, and the gas is assumed to be ideal). The fact that p_v is underestimated by both models can be linked to the overestimation of ΔH_v (12.9 kcal/mol for OPC, 11.99 kcal/mol for TIP4P/2005, and 10.5 kcal/mol for the experiment). Yielding higher values of ΔH_v means that the energies of the liquid are over-estimated (in absolute value, that is, that the energy of the liquid is more negative than the experimental one). The same is true for its chemical potential (μ). At coexistence, μ is equal for both phases, and in the case of the vapor, it can be treated as an ideal gas [so $\mu \approx k_B T \ln(\rho)$]. Since we have established that the chemical potential of the model is underestimated, the density of the gas is underestimated too [$\exp(\mu/k_B T) \approx \rho$], and the same happens for the vapor pressure. Thus, larger vaporization enthalpies imply lower vapor pressures. This is precisely what is observed in Fig. 3. At this point, it is worth mentioning that TIP3P, TIP4P, or TIP5P models, which reproduce the vaporization enthalpy of water at room temperature, significantly underestimate the critical temperature of

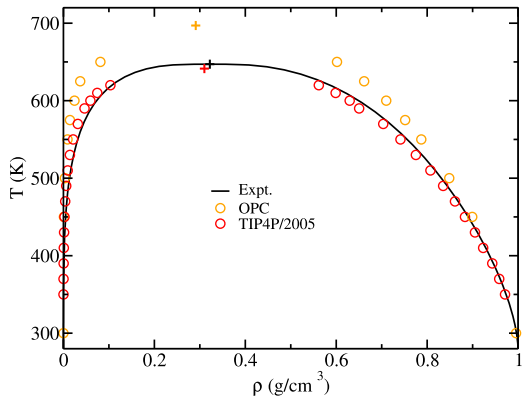

FIG. 1. Coexistence densities of the vapor–liquid equilibria for the OPC model compared with the TIP4P/2005 (from Ref. 63) and experimental results from Ref. 92.

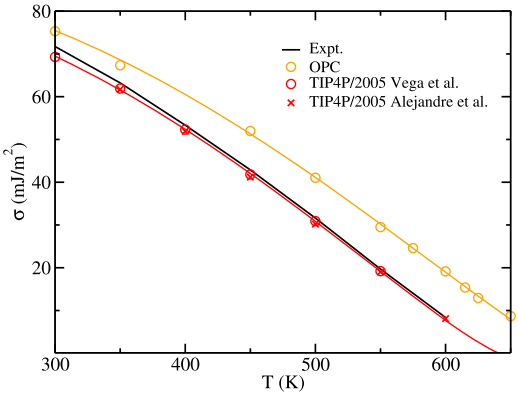

FIG. 2. Surface tension of water for the OPC (this work) and the TIP4P/2005 (circles from Ref. 64 and crosses from Ref. 93) compared with experimental data (from Refs. 94 and 95). Fits to the simulation results were obtained from Eq. (6).

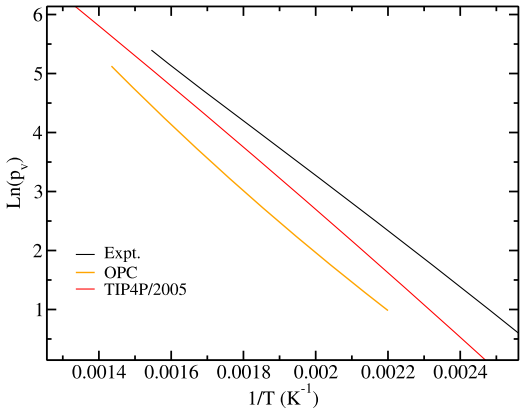

FIG. 3. Fits to the vapor pressure (in bar) using Eq. (7) for the OPC (this work) compared with the TIP4P/2005 (from Ref. 63) and experimental results (from Ref. 103).

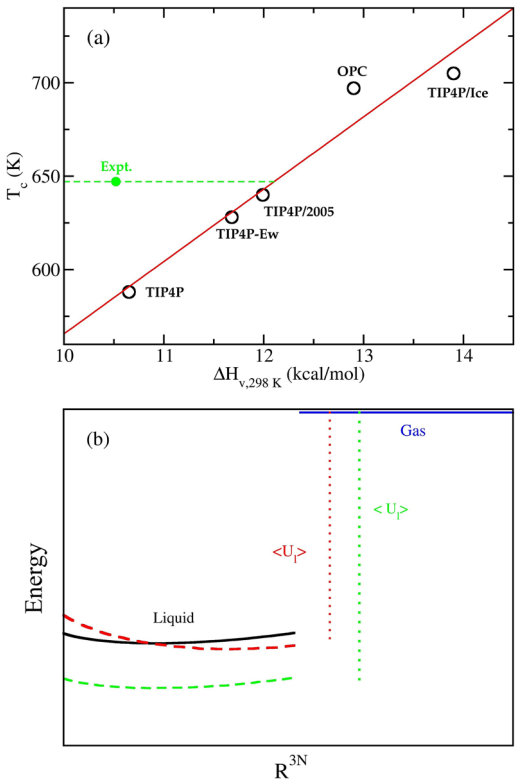

FIG. 4. (a) Correlation between the critical temperature (T_c) and the vaporization enthalpy at 298 K ($\Delta H_{v,298K}$) for several rigid four-centered non-polarizable models: TIP4P from Ref. 102, TIP4P-Ew from Refs. 38 and 63, OPC (this work), and TIP4P/2005 and TIP4P/Ice from Refs. 29 and 63. The red line shows a linear correlation between both properties. The green point depicts the experimental value of the vaporization enthalpy and the critical point, and the green dashed line interception with the red line provides the optimal value of ΔH_v for reproducing T_c with 4C non-polarizable models. (b) Sketch (adapted from Ref. 53) of the PES for the liquid (black solid line) and for the vapor (blue solid line) as a function of phase space obtained from first principles. The red dashed line represents the energies of the liquid for a model that reproduces the absolute values of the potential energy (as, for instance, TIP4P) and the vaporization enthalpy (red dotted curve plus the RT contribution coming from the pV term of the gas), whereas the green dashed line depicts a model able to capture the gradient of the potential energy (e.g., TIP4P/2005) but not the vaporization enthalpy (green dotted curve plus RT). Vertical lines represent the mean value of the potential energy ($\langle U_l \rangle$), it being one of the main contributions to the vaporization enthalpy ΔH_v.

water, T_c (by about 80 K). On the other hand, models overestimating ΔH_v yield closer values to the experimental one (SPC/E underestimates T_c by 25 K and TIP4P/2005 only by 4 K). Therefore, since ΔH_v is higher for the OPC model than for TIP4P/2005, it is not surprising that the former overestimates the critical temperature by 50 K. For rigid non-polarizable models, there exists a correlation between the value of the vaporization enthalpy and the critical temperature. Guillot initially observed this phenomenon for several rigid non-polarizable models.[104] We depict this correlation in Fig. 4(a) for various 4C models. It is shown that a value of ~12 kcal/mol is considered the optimal choice for accurately reproducing the critical point. Berendsen and co-workers were the first ones using this approach implicitly, as SPC/E[26] is indeed a better model than SPC even though it overestimates the vaporization enthalpy. However, the use of Berendsen's correction to the vaporization enthalpy in a water model does not guarantee a good critical temperature. This is exemplified by the fact that although Berendsen's correction was implicitly taken into account when designing the OPC model, this model still considerably overestimates T_c [Fig. 4(a)]. Regarding the value of the corrected enthalpy of vaporization, Berendsen's correction[26] should be treated with caution, as it is not universally accepted. Leontyev and Stuchebrukhov showed that the polarization correction as implemented by Berendsen *et al.* is not totally consistent since it uses the dipole moment of the model of water (which is incorrect) and not the actual dipole moment of water in the liquid state.[47] Using the value of real water's dipole moment in Berendsen's corrections would lead to an extremely large and positive polarization correction. These authors[46] along with Jorge and co-workers[19,105] argue that the polarization correction has two contributions, namely, the distortion correction (which is positive) as given by Berendsen's expression but using the actual dipole moment of water, and the electronic screening correction, which is of opposite sign so that the sum of both terms is very small and positive. Furthermore, some of the present authors have recently proposed a new type of correction to the vaporization enthalpy and the hydration free energy of water.[106] It involves computing the chemical potential and partial molar enthalpy of a "test particle," specifically a modified TIP4P-2005 particle (denoted as an ECS molecule with charges 3.5% lower than the original model). This is done within a fluid of TIP4P/2005 molecules for each thermodynamic state resulting in an excellent description of these two properties up to the critical temperature. The tendency of early water models to accurately reproduce the enthalpy of vaporization is primarily due to the fact that this property is easily accessible experimentally and straightforward to calculate computationally. However, attempting to reproduce it with a classical model can be conceptually flawed because these models, lacking electrons, are unable to account for the change

in internal energy that occurs due to the reorganization of electron clouds during the phase change. Therefore, necessarily, reproducing this property will entail a trade-off with other properties. This is schematically and rather intuitively represented in panel (b) of Fig. 4. The black solid line represents the energy of liquid water (as would be obtained by exactly solving the Schrödinger equation) as a function of the positions of the molecules (represented by R^{3N}). In the red dashed line, the energy of the liquid is shown for a model that yields values similar to those of real water for a certain configurational space, deviating slightly in neighboring phase spaces. The dotted lines represent the average potential energy (the residual contribution to the internal energy) of the liquid in the configurational space. Therefore, the model described in red will be able to provide an appropriate value for the enthalpy of vaporization, as the energy of the gas phase is close to zero. In green (dashed line), another model is shown, which systematically underestimates the energy of the liquid but is parallel to it. Evidently, this model overestimates the enthalpy of vaporization. However, simulations of the system with the black solid curve (exact energies) and with the green dashed curve will generate identical trajectories and, therefore, identical transport and thermodynamic properties (energies differing by a constant value), as in simulations only relative energies between configurations (i.e., Monte Carlo technique) or forces (i.e., gradient of the energy) are relevant. Of course, this sketch is an idealization (the green dashed curve is exactly parallel to the solid curve in our example), but it illustrates the point. TIP4P behaves as the red dashed curve, and TIP4P/2005 behaves as the green dashed curve (although, of course, it is not exactly parallel to the solid curve). This reasoning was already mentioned in Ref. 53 and is further expanded here. We believe that the success of TIP4P/2005, where relative energies (not absolute energies) between configurations are better represented, might be due to the correlation between the enthalpy of vaporization and the critical temperature shown in panel (a) of Fig. 4 since the latter, representing a limit in the phase diagram, is a key feature of a good-performing model.

In conclusion, in terms of liquid–vapor properties, the TIP4P/2005's "weak spot" is undoubtedly the vapor pressure. Consequently, the fact that the predictions for p_v provided by the OPC lie even further away from the experiments along with its overestimation of T_c and σ results in this model yielding worse estimates for the critical properties and for the liquid–vapor equilibrium, generally speaking. This difference in performance can be easily observed in Tables II and III.

We now introduce the melting and ices properties. In 2020, Onufriev and co-workers reported a melting point for the OPC model of 242.1 K using the direct coexistence technique.[107] In this work, we have also conducted direct coexistence simulations for the OPC, as depicted in Fig. 5, obtaining a melting temperature (T_m) of 244.5 K. Both values concur within the error bar. The melting point for the TIP4P/2005 model is higher (250 K[36,108]) and closer to the experimental melting point of ice (273 K). As a matter of fact, both models exhibit large deviations from the experimental behavior. This is because they were parameterized to reproduce the TMD. As we have already mentioned, these two temperatures are correlated and, for non-polarizable models, exhibit a difference of around 25 K,[31,36] as compared to the experimental difference of 4 K.

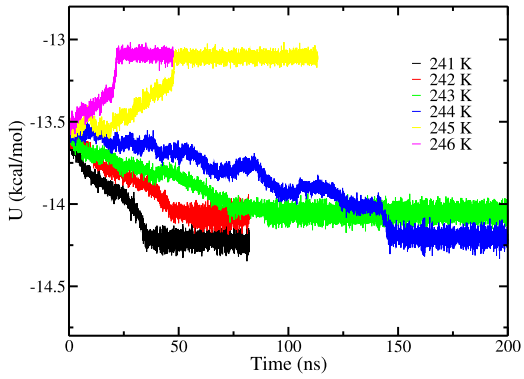

FIG. 5. Evolution of the potential energy as a function of time for direct coexistence (water-I_h) NpT simulations for the OPC model at 1 bar and different temperatures.

Concerning the melting enthalpies (ΔH_m), both models underestimate the experimental value (see Table II), with OPC showing a slightly larger deviation. Additionally, OPC significantly underestimates the density of ice Ih, which has consequences regarding the (i.e., dp_{melt}/dT) of the melting curve. The experimental slope is about −140 bar/K, whereas we have estimated −90 bar/K for OPC and −132 bar/K for TIP4P/2005. Therefore, the melting temperature of ice Ih for OPC will change much more with pressure when compared to the experimental findings (due to its larger dT_{melt}/dp value).

Let us turn our attention to the discussion of the densities of ice polymorphs for each model under investigation. While the liquid phase of water has often been the focus of extensive studies, many authors have insisted upon the relevance of ices when developing water potential models.[34,109,110] In addition, recent years have seen a growing interest in the simulation of ice and gas hydrates.[12,14,111–115] Therefore, we believe that an accurate model should also extend its descriptive capabilities to various ice polymorphs. Our examination focuses on densities due to their simplicity in both experimental and simulation measurements. We shall consider an ice with proton order (ice II) and ices with proton disorder, such as Ih, V, and VI. We used the algorithm of Buch *et al.*[116] to generate the proton disorder. Looking at the results in Table II, it becomes evident that the TIP4P/2005 model closely aligns with experimental densities for all the studied ice polymorphs (I_h, II, V, and VI). In contrast, the OPC model shows bigger deviations from experiments.

In our exploration of densities under different conditions, we also delved into the Equation of State (EOS) of liquid water at high pressures for an isotherm (373 K). The results presented in Table II demonstrate that at both pressures (10 and 20 kbar), the TIP4P/2005 model outperforms the OPC model. The latter notably underestimates densities in both cases.

This comparison highlights a consistent trend: the OPC model fails in describing the densities of various ice polymorphs and liquid water under high-pressure conditions obtaining scores of 4.8 and 7.5, respectively (see Table III). In contrast, the TIP4P/2005 model consistently reproduces the experimental observations scoring 8.3 and 10, thus showing its robust performance across different scenarios.

As previously discussed, water models developed in the 2004–2005 period, exemplified by TIP4P/2005[39] and TIP4P/Ew,[38] were aimed at reproducing the TMD and incorporated the idea of the self-polarization energy implicitly by not targeting the vaporization enthalpy. In a recent study, we conducted a precise evaluation of the TMD for TIP4P/2005,[117] obtaining a value of 277.3 K, which remarkably aligns with the experimental TMD of water at 277 K. Subsequently, in this work, we have extended this analysis to accurately assess the TMD of the OPC model. Figure 6 displays the densities of both models as a function of temperature. The results indicate that they effectively replicate the densities of liquid water at room temperature. However, a noticeable distinction emerges at lower temperatures, where the performance of TIP4P/2005 clearly surpasses that of the OPC. The outcome reveals that the density curvature of the TIP4P/2005 is able to reproduce the experimental one at least down to 240 K, whereas the OPC's curvature flattens below the TMD, resulting in a progressive overestimation of the density as the temperature decreases. This might be extremely relevant for studies of supercooled water,[61,118] which have become very popular since the ground-breaking study of Speedy and Angell[119] and the following literature on the matter.[3,6,120] The incorrect prediction of the curvature by the OPC below 280 K results in a TMD of 270.1 K, lower than the experimental value of 277 K and below that of TIP4P/2005 model (277.3 K). It is worth mentioning that seven degrees is still a small deviation for the TMD, considering that most 3C models underestimate it by more than 20 K.[36] Even some polarizable models fail in reproducing this property, such as MB-Pol[121–123] that underestimates the TMD by 12 K or AMOEBA,[124] which exhibits it 13 K above the experimental result.[125]

Once the values of the melting temperature (T_m), maximum in density (TMD), and critical temperature (T_c) are determined, we can analyze what could be referred to as the "phase diagram aspect" by evaluating the ratios between these temperatures (see Table II). Overall, these ratios appear to be better described by TIP4P/2005. However, the experimental difference of 4 K between the TMD and the melting temperatures is not well described by either OPC or TIP4P/2005. This failure seems to be a common mistake for all 3C and 4C non-polarizable water models.[31] However, this difference is considerably reduced with polarizable models, such as MB-Pol.[36,121,122]

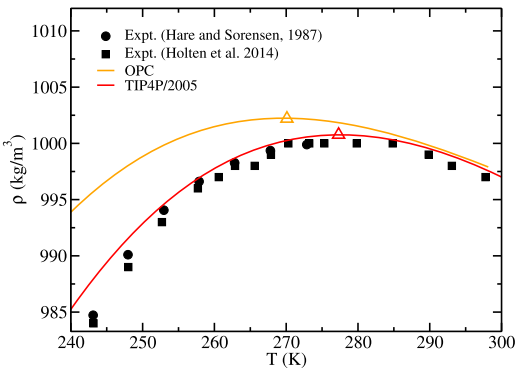

FIG. 6. Density of liquid water as a function of temperature at p = 1 bar obtained using the TIP4P/2005 (from Ref. 117) and OPC models. The experimental results were taken from Refs. 126 and 127. Solid lines are cubic fits to the simulation points (see the text), and empty triangles represent the temperature of maximum density.

Regarding the transport properties of liquid water, we provide the viscosity and diffusion coefficients at different temperatures, which are collected in Table II. Our viscosities for OPC are consistent with those recently reported by Ando.[128] It is apparent that both models yield viscosity values that closely align with the experimental data at the three temperatures examined, although the TIP4P/2005 results exhibit a slight superiority over those of the OPC model. When considering diffusion coefficients, the conclusions are similar, and TIP4P/2005 shows a slightly better performance than the OPC model. In addition, the TIP4P/2005 model also gives a better estimate of the Arrhenius activation energy. However, both models provide a good agreement with the reported experimental values. In fact, the performance of both TIP4P/2005 and OPC when describing transport properties is notably commendable.

As for the heat capacities (C_p) of liquid water, both models overestimate the experimental value, being the results provided by the OPC superior to those of TIP4P/2005. For the solid phase, this property is not well reproduced by either of them. As it has been discussed in a previous work,[129] nuclear quantum effects are needed to estimate heat capacities, and hence, non-polarizable (or even polarizable) models are not expected to describe the experimental heat capacities.

In the original VA-Test, the phase diagram (including solid–solid and solid–fluid transitions) was determined. Nevertheless, due to the difficulty of numerically evaluating it, this only contributed with approximately a 6% to the total score of the VA-Test. Obtaining the entire phase diagram of the OPC model is beyond the scope of this work. However, we expect the phase diagrams of OPC and TIP4P/2005 not to be dramatically different. This is induced by the fact that the phase diagram for the TIP4P/Ice, which has recently been calculated by Paesani and co-workers,[130] exhibits a significant resemblance to that of TIP4P/2005.[131] Furthermore, Abascal and Vega showed that TIP4P-like geometry displays qualitatively similar phase diagrams, which are shifted from each other with a strong dependence on the dipole–quadrupole ratio.[35] Therefore, it is reasonable to assume that the numerical scores of OPC and TIP4P/2005 in the VA-Test for the phase diagram would not have differed much from each other. Thus, we do not expect the final score of the VA-Test to have been impacted by the inclusion of the OPC's phase diagram had this property been computed (although further work is needed to confirm this). The same is true for the structure. In the supplementary material, we collect the radial distribution functions (RDFs) for the oxygen–oxygen (OO) and oxygen–hydrogen (OH) for liquid water at room temperature and that of ice Ih at 220 K for both models and compare them with experimental results.[132–134] Structural predictions are rather similar for both potentials, being almost identical for ice Ih, slightly better for the OPC regarding the oxygen–oxygen radial distribution function of water (see the first minimum) and slightly better for TIP4P/2005 when describing the oxygen–hydrogen radial distribution function of water (see the first maximum).

Finally, we address the results for the dielectric constant of liquid water. Not surprisingly, since ε_r was used as a target property when developing the OPC, this model reproduces the experimental value (i.e., 78), whereas the prediction of TIP4P/2005 is considerably lower (i.e., 57). Although we have not computed the dielectric constant of ice Ih for OPC as its calculation requires special methods to sample the proton disorder,[54] it would be interesting to determine it in the future. Even more so, considering that some models that provided a good dielectric constant for liquid water (as TIP5P) gave very poor estimates of ε_r for ices.[54]

Once all the results for the TIP4P/2005 and OPC models have been presented in Table II, it is time to calculate the final score, which is shown in Table III. TIP4P/2005 obtains a mark of 7.2 (identical to that reported in 2011), whereas OPC scores 6.3. Certainly, OPC obtains a higher grade than models developed more than a decade before, such as TIP3P (2.7), TIP5P(3.7), TIP4P(4.7), and SPC/E (5.1). However, it does not outperform TIP4P/2005, but rather falls short by around a point in the score, a significant difference. Thus, the results of this work support the idea that using the dielectric constant as a target property for non-polarizable models does not globally improve the description of water, but rather the opposite, it somewhat deteriorates the overall performance as compared to models that provide a lower ε_r value than the experimental one. There is no such thing as a free lunch: the attempt to enhance the prediction of the dielectric constant worsens the description of many other properties of water.

Is there an explanation to this finding? The first point to notice is that the dielectric constant is qualitatively different from the rest of the properties shown in Table II. When solving the Schrödinger equation for a certain nuclear configuration, the energy of the system is obtained. The function that describes how the energy of the system changes with the position of the nuclei is denoted as the PES. The knowledge of this surface is sufficient to determine all properties shown in Table II but one: the dielectric constant. For computing ε_r, the polarization of each configuration must be known (i.e., the global dipole moment).[53] The function describing the changes of polarization with the position of the nuclei is known as the dipole moment surface (DMS). Quantum calculations enable the evaluation of the energy (PES) and the dipole moment (DMS) of each configuration. For decades, it has been assumed that the charges used by empirical models to describe the PES should also be employed for the DMS.[53] We advocate that this is not correct. Quite recently, the dielectric constant of water has been determined from quantum calculations by using two different neural networks (one for the PES and another for the DMS[52]). It is agreed upon that the charges used to fit the PES in non-polarizable force fields are empirical parameters (since point charges are not observable) and do not entail any specific physical meaning, therefore enabling for a different set of charges to describe the DMS. In fact, a recent study by Cardona *et al.*[135] proved that simple corrections accounting for electronic polarization effects recover the static dielectric constant as a function of temperature for two non-polarizable rigid water models and its binary mixtures with alcohols. A more sophisticated approach along the same lines has been recently addressed by Han *et al.*[136] in an interesting paper, showing that polarization and charge transfer obtained from quantum calculations can be incorporated to TIP4P/2005 MD trajectories via machine learning to reproduce the experimental value of the dielectric constant of water and the hydrogen-stretch peak in the IR spectrum.

Generally, the properties that require both surfaces to be computed are response functions of a system to the application of an electric external field. The electrical conductivity, as well as the dielectric constant, clearly fit this description. In the absence of an external electric field, all the properties studied in this work with the exception of the dielectric constant can be evaluated from the PES only. The dipole moment that correctly reproduces this surface is in the range of 2.3–2.4 D, whereas the dipole moment of "real" water in the liquid phase, estimated from reasonable methods for partitioning the electronic cloud, typically falls within the range of 2.8–3.0 D.[48–52] As previously discussed (see Sec. I), Leontyev and Stuchebrukhov[45,46] suggested a dipole moment of 2.2 D for water to characterize the PES, which would yield a dielectric constant of 45. While we acknowledge the argument put forward by them as a guiding principle, we believe that there are certain degrees of freedom in determining the precise values to be employed. Consequently, TIP4P/2005 incorporates a dipole moment of 2.3 D and a dielectric constant of 57.

The reader may feel uncomfortable about our statement that the dielectric constant is relevant only in the presence of an external electric field. However, this is certainly the case as can be consulted in any book of electromagnetism:[137] the dielectric constant is defined and measured as the response of a system (polarization) to an external electric field. If there is no electric field, the dielectric constant is irrelevant. However, the reader may argue an exception: electrolyte solutions. In the presence of ions, there is no external field, and yet, the dielectric constant is apparently needed to properly define the system. To answer this apparent dilemma, let us introduce the potential of mean force $w(r)$, which is defined by the following expression:[138]

$$g(r) = \exp\left(\frac{-w(r)}{k_B T}\right), \tag{13}$$

where $g(r)$ is the radial distribution function. For a 1:1 electrolyte at infinite dilution, it can be shown that at the limit of very large distances, $w(r)$ for the ion–ion distribution function behaves in the following way:[139]

$$w(r) = \frac{e \cdot e}{4\pi\epsilon_0\varepsilon_r r}, \tag{14}$$

where e is the charge of the electron and ε_0 is the permittivity of the vacuum. The thermodynamic properties of highly diluted solutions are dominated by the behavior of $g(r)$ at very large distances. The Debye–Hückel theory (DH) provides the exact activity coefficient γ (also referred to as mean ionic activity coefficient) for a 1:1 solution at very high dilution as

$$\log_{10}(\gamma) = -Am^{1/2}, \tag{15}$$

being m the molality (i.e., mol of salt per kg of water) and A[140–142] a constant obtained (using the international system of units) as

$$A = \frac{e^3\sqrt{2N_A\rho_{H_2O}}}{8\pi\ \ln(10)(\varepsilon_0\varepsilon_r k_B T)^{3/2}}, \tag{16}$$

TABLE IV. Values of constant A corresponding to the Debye–Hückel law (at room p and T) as obtained from experiment (Ref. 140), for OPC, TIP4P/2005, and ECCw2024 using different values of λ. The first set of results shows the "natural value" of λ for each model (the one needed to recover the experimental A coefficient). The second set of results displays different choices of λ yielding values of A that deviate from experiments.

Water	ε_r	λ	J	A
Exp.	78.4	1	78	0.51
OPC	78	1	78	0.51
TIP4P/2005	57	0.85	79	0.51
ECCw2024	44.3	0.75	79	0.51
OPC	78	0.85	108	0.31
OPC	78	0.75	139	0.22
TIP4P/2005	57	1.00	57	0.82
TIP4P/2005	57	0.75	101	0.35
ECCw2024	44.3	1.00	44.3	1.20
ECCw2024	44.3	0.85	61	0.74

where N_A is the Avogadro number and ρ_{H_2O} is the mass density of pure water (in kg/m^3). Two key properties are needed in order to reproduce the experimental value of A: the density and the dielectric constant of pure water. The former is well described by most water models (at least at room conditions), whereas the latter is only accurately reproduced by non-ECC models. Bearing this in mind, are ECC models able to describe the value of the DH constant A? Let us rewrite Eq. (14) scaling the charge by a factor λ,

$$w(r) = \frac{\lambda e \cdot \lambda e}{4\pi\varepsilon_0\varepsilon_r r} = \left(\frac{\varepsilon_r}{\lambda^2}\right)^{-1} \frac{e^2}{4\pi\varepsilon_0 r} = J^{-1}\frac{e^2}{4\pi\varepsilon_0 r}, \tag{17}$$

where J is

$$J = \frac{\varepsilon_r}{\lambda^2} \tag{18}$$

and the expression for A is now written as

$$A = \frac{e^3\sqrt{2N_A\rho_{H_2O}}}{8\pi\ln(10)(\varepsilon_0 J k_B T)^{3/2}}. \tag{19}$$

The conclusion of Eqs. (17) and (19) is that two force fields with the same value of J will also have the same potential of mean force and the same limiting Debye–Hückel law. The experimental value of A (at room T and p) is recovered with the choice $\lambda = 1$ and $\varepsilon_r = 78.4$. Thus, OPC, which reproduces the experimental value of the dielectric constant of water, obeys the experimental DH law when choosing a force field for the ions with $\lambda = 1$. However, the experimental value of A can also be described by using the TIP4P/2005 model ($\varepsilon_r = 57$) and $\lambda = 0.85$ or the ECCw2024 model[41] ($\varepsilon_r = 45$) and $\lambda = 0.75$. This can easily be observed in Table IV. Thus, a correct description of the dielectric constant is not indispensable to reproduce the DH experimental limiting law, as long as scaled charges are included.

The idea that there is a "natural value" of λ for each potential model of water was first exposed by Kann and Skinner.[71] In Table IV, we have also included the values of A obtained when λ differs from the "natural choice" in order to emphasize the resulting deviations from the DH law in such cases.

It should be reminded that the DH law is exact only at very low concentrations (well below 0.1 m). Above this limit, a correct value of ε_r does not guarantee a good description of the electrolytes in water[143] (i.e., activity coefficients, densities, transport properties, and osmotic pressures). This is not shocking since even for a 1 m solution, there are ~27 molecules of water per ion (first and second solvation shells), and therefore, the potential of mean force between ions can no longer be obtained from the Coulomb law. Note that the scaling of ions is a common practice within the ionic liquids community.[144–148] Recently, some groups have extended this idea to electrolyte solutions as well, such as Kann and Skinner,[71] ourselves,[149] Predota and co-workers,[150] Jungwirth and co-workers,[151,152] Alejandre and co-workers,[153] and Barbosa and co-workers,[154] although admittedly, the majority of the community still stands for the choice of $\lambda = 1$.

IV. CONCLUSIONS

A long effort has been undertaken to improve water models since the seminal work of Bernal and Fowler in 1933.[20] One approach to "quantify" such improvement was developed by Vega and Abascal in 2011 (VA-Test).[29] They achieved this by evaluating numerous properties across various thermodynamic states of water, encompassing all its phases. From that thorough work, the superiority of 4 center (4C) geometry over 3 center (3C) and 5 center (5C) was established, a finding that has been subsequently corroborated by other authors.[33,67] Furthermore, the necessity of employing Ewald sums to accurately account for electrostatic interactions, the advantage of utilizing models that overestimate the experimental value of water's vaporization enthalpy (as initially proposed by Berendsen *et al.*[26]), and the significance of reproducing the temperature of maximum density (TMD) of water (as first suggested by Mahoney and Jorgensen[30]) were all proven to be sound concepts. Considerable deviations from experimental values were particularly evident in gas/vapor properties, virial coefficients, heat capacities, enthalpies of phase change, and the dielectric constant. These discrepancies highlight the limitations of non-polarizable models in accurately describing the properties of real water.

With the dielectric constant (ε_r) consistently underestimated by a substantial margin across all previously developed models, the last decade has seen the emergence of numerous models that retain earlier concepts but prioritize achieving an accurate dielectric constant. The deviation between the dielectric constant of non-polarizable models and experiments does not constitute a mere parameterization effort, but rather implies an important conceptual subtlety. As Leontyev and Stuchebrukhov pointed out in their Electronic Continuum Correction (ECC) theory,[45–47] the value of the dielectric constant at high frequencies $\epsilon_{r,\infty}$ (where only electrons can be accommodated as a response the external field) cannot be reproduced by classical simulations. Therefore, in this context, the appropriate dielectric constant of water should be rescaled according to a significant lower value. Vega proposed a similar

approach,[53] indicating that the dielectric constant should account for variances in the optimal dipole moments necessary to characterize both the PES (2.2–2.3 D) and the DMS surfaces (2.8–3.0 D). This idea constitutes the foundational underpinning of several successful models devised during the mid-2000s (ECC models), such as TIP4P-Ew[38] or TIP4P/2005,[39] and others introduced more recently, for instance, TIP4P-D[40] and ECCw2024.[41] The ECC approach for developing force fields has also been advocated by Jorge and co-workers[56,57] and Jungwirth and co-workers.[41] Note that this is diametrically opposed to the purpose of using the dielectric constant as a target property in the parameterization of rigid non-polarizable water models (non-ECC approach). In this work, we have compared the performance of TIP4P/2005 and OPC as case studies of the ECC and non-ECC approaches (respectively) by implementing the VA-Test. The comparison primarily entailed reanalyzing previously published results of the TIP4P/2005 model, supplemented by newly computed properties for the OPC model. Specifically, the liquid–vapor equilibria, interfacial tension, ice polymorphs densities, and equations of state (EOS) at high pressure are noteworthy as they have not been previously reported for this model. Additionally, the melting point, the temperature of maximum density (TMD), and the response functions (isothermal compressibility and heat capacities) were accurately recomputed. Although the target properties of both models are not identical and that could slightly affect the final score, the key difference between both models is the inclusion (OPC) or not (TIP4P/2005) of the dielectric constant as a target property.

Employing the VA-Test, a global mark of 6.3 was obtained for the OPC model, whereas the TIP4P/2005 scored 7.2. With this comprehensive comparison, we have proved that TIP4P/2005 is more suited for representing the properties of water in different phases and thermodynamic states than the non-ECC model under consideration: OPC. Thus, we draw the conclusion that water potentials that aim at enhancing the dielectric constant of water do not provide a better description of the PES than those that underestimate ε_r.

Rome was not built in a day, and, as we have seen, neither were water models. Let us briefly draw a parable. We will enumerate the main achievements regarding the modeling of non-polarizable water in the past century. Each of these contributions can be regarded as a conceptual block for building a suitable non-polarizable model:

- Setting a 4C geometry.
- Overestimating the vaporization enthalpy of water when determining the parameters of the force field.
- Reproducing the maximum in density.
- Using Ewald sums for treating the electrostatic interactions.
- Adopting the electronic continuum correction by underestimating the dielectric constant.

It seems that all the bricks have been laid out, and we have reached the pinnacle of development for non-polarizable water models. It is astonishing how many properties these simple models can accurately describe. However, we must humbly acknowledge that they cannot replicate all experimental properties of water, and there is not much scope for further improvement in non-polarizable models, being TIP4P/2005 close to the limit of what can be obtained. Of course, force fields with specific aims (reproducing a limited set of properties) can still be developed, as, for instance, TIP4P/Ice, which correctly describes the melting point of hexagonal ice,[155] or the coarse grained mW model of Molinero and co-workers[156] enabling fast simulations of very large systems. However, these special purpose models would not obtain a higher score in the VA-Test. Not surprisingly, it is not feasible to reproduce all the properties of water with such a simple description; it is indeed remarkable how far we have traveled in the last century.

Finally, the choice between ECC and non-ECC models of water affects the choice of the charge assigned to the ions in water when modeling electrolytes, particularly if the exact Debye–Hückel limiting law is to be recovered. For non-ECC models, integer charges in electron units must be used, whereas for ECC models, scaled charges are needed, which are becoming increasingly popular.[71,150–154,157] Certainly, one could choose to disregard the Debye–Hückel law, for instance, by employing scaled charges for ions along with water models describing the dielectric constant of water. However, this would open a can of worms: what then would have been the purpose of reproducing the dielectric constant of water in the first place?

In order to overcome the undeniable shortcomings of non-polarizable models, the development of polarizable force fields has accelerated in recent years. Some examples are the BK3,[32] i-AMOEBA,[158] HBP,[159] MB-Pol,[121,122,160] and q-Aqua.[161] It is likely that these models would obtain a higher score than TIP4P/2005 in the VA-Test, although some polarizable force fields cast serious doubts on whether they outperform the best non-polarizable ones.[136,162] On top of that, neural networks[163,164] also emerged as a plausible alternative. Some many-body polarizable potentials show quite promising results in the overall description of water properties;[32,69,122,161,165] however, due to their high computational cost, they cannot be applied to the study of high-demanding simulations. In any case, it seems that non-polarizable models, with their intrinsic limitations, still have a significant lifespan among us, as they may suffice to describe the essential physics of many interesting problems.

SUPPLEMENTARY MATERIAL

In the supplementary material, we collect the numerical data for the surface tension, vapor pressure, and liquid and vapor densities of the liquid–vapor equilibria for the OPC model. Numerical data for the densities at 1 bar and different temperatures for OPC and TIP4P/2005 are also presented. We also show a comparison between experiment and simulations for both models for the oxygen–oxygen and oxygen–hydrogen radial distribution functions (for water and ice Ih).

ACKNOWLEDGMENTS

This work was funded by Grant No. PID2022-136919NB-C31 of the MICINN. L.F.S. acknowledges the Ministerio de Educacion y Cultura for a pre-doctoral FPU under Grant No. FPU22/02900. S.B. acknowledges Ayuntamiento de Madrid for a Residencia de Estudiantes grant. The authors would also like to express their gratitude to Javier Oller for his help with the table of contents graphical abstract.

AUTHOR DECLARATIONS

Conflict of Interest

The authors have no conflicts to disclose.

Author Contributions

L. F. Sedano: Data curation (equal); Formal analysis (equal); Investigation (equal); Methodology (equal); Writing – original draft (equal); Writing – review & editing (equal). **S. Blazquez**: Data curation (equal); Formal analysis (equal); Investigation (equal); Methodology (equal); Writing – original draft (equal); Writing – review & editing (equal). **C. Vega**: Conceptualization (equal); Data curation (equal); Formal analysis (equal); Funding acquisition (equal); Investigation (equal); Supervision (equal); Writing – original draft (equal); Writing – review & editing (equal).

DATA AVAILABILITY

The data that support the findings of this study are available within the article and in the supplementary material.

REFERENCES

[1] P. Ball, *Life's Matrix. A Biography of Water* (University of California Press, Berkeley, 2001).
[2] P. G. Debenedetti, J. Phys.: Condens. Matter **15**, R1669 (2003).
[3] P. Gallo, K. Amann-Winkel, C. A. Angell, M. A. Anisimov, F. Caupin, C. Chakravarty, E. Lascaris, T. Loerting, A. Z. Panagiotopoulos, J. Russo *et al.*, Chem. Rev. **116**, 7463 (2016).
[4] L. G. M. Pettersson, R. H. Henchman, and A. Nilsson, Chem. Rev. **116**, 7459 (2016).
[5] T. C. Hope, Trans. R. Soc. Edinburgh **5**(2), 379–405 (1805).
[6] P. G. Debenedetti and F. H. Stillinger, Nature **410**, 259 (2001).
[7] D. Marx and M. Parrinello, J. Chem. Phys. **104**, 4077 (1996).
[8] K. Burke, J. Chem. Phys. **136**, 150901 (2012).
[9] A. D. Becke, J. Chem. Phys. **140**, 18A301 (2014).
[10] M. Karplus and G. A. Petsko, Nature **347**, 631 (1990).
[11] S. Blazquez, I. Sanchez-Burgos, J. Ramirez, T. Higginbotham, M. M. Conde, R. Collepardo-Guevara, A. R. Tejedor, and J. R. Espinosa, Adv. Sci. **10**, 2207742 (2023).
[12] E. Sanz, C. Vega, J. Espinosa, R. Caballero-Bernal, J. Abascal, and C. Valeriani, J. Am. Chem. Soc. **135**, 15008 (2013).
[13] A. Haji-Akbari and P. G. Debenedetti, Proc. Natl. Acad. Sci. U. S. A. **112**, 10582 (2015).
[14] J. Grabowska, S. Blazquez, E. Sanz, E. Noya, I. M. Zerón, J. Algaba, J. M. Míguez, F. J. Blas, and C. Vega, J. Chem. Phys. **158**, 114505 (2023).
[15] S. Harrington, R. Zhang, P. H. Poole, F. Sciortino, and H. E. Stanley, Phys. Rev. Lett. **78**, 2409 (1997).
[16] J. C. Palmer, F. Martelli, Y. Liu, R. Car, A. Z. Panagiotopoulos, and P. G. Debenedetti, Nature **510**, 385 (2014).
[17] P. G. Debenedetti, F. Sciortino, and G. H. Zerze, Science **369**, 289 (2020).
[18] M. A. González and J. L. F. Abascal, J. Chem. Phys. **135**, 224516 (2011).
[19] A. W. Milne and M. Jorge, J. Chem. Theory Comput. **15**, 1065 (2019).
[20] J. D. Bernal and R. H. Fowler, J. Chem. Phys. **1**, 515 (1933).
[21] J. A. Barker and R. O. Watts, Chem. Phys. Lett. **3**, 144 (1969).
[22] A. Rahman and F. H. Stillinger, J. Chem. Phys. **55**, 3336 (1971).
[23] F. H. Stillinger and A. Rahman, J. Chem. Phys. **60**, 1545 (1974).
[24] H. J. C. Berendsen, J. P. M. Postma, W. F. van Gunsteren, and J. Hermans, *Intermolecular Forces* (Reidel, Dordrecht, 1981).
[25] W. L. Jorgensen, J. Chandrasekhar, J. D. Madura, R. W. Impey, and M. L. Klein, J. Chem. Phys. **79**, 926 (1983).
[26] H. J. C. Berendsen, J. R. Grigera, and T. P. Straatsma, J. Phys. Chem. **91**, 6269 (1987).
[27] W. M. Jones, J. Chem. Phys. **48**, 207 (1968).
[28] M. M. Popov and F. I. Tazetdinov, Sov. J. At. Energy **8**, 353 (1961).
[29] C. Vega and J. L. F. Abascal, Phys. Chem. Chem. Phys. **13**, 19663 (2011).
[30] M. W. Mahoney and W. L. Jorgensen, J. Chem. Phys. **112**, 8910 (2000).
[31] C. Vega and J. L. F. Abascal, J. Chem. Phys. **123**, 144504 (2005).
[32] P. T. Kiss and A. Baranyai, J. Chem. Phys. **138**, 204507 (2013).
[33] C. Vega, J. L. F. Abascal, E. Sanz, L. G. MacDowell, and C. McBride, J. Phys.: Condens. Matter **17**, S3283–S3288 (2005).
[34] C. Vega, J. L. F. Abascal, M. Conde, and J. Aragones, Faraday Discuss. **141**, 251 (2009).
[35] J. L. F. Abascal and C. Vega, J. Phys. Chem. C **111**, 15811 (2007).
[36] S. Blazquez and C. Vega, J. Chem. Phys. **156**, 216101 (2022).
[37] D. Frenkel and B. Smit, *Understanding Molecular Simulation* (Academic Press, London, 1996).
[38] H. W. Horn, W. C. Swope, J. W. Pitera, J. D. Madura, T. J. Dick, G. L. Hura, and T. Head-Gordon, J. Chem. Phys. **120**, 9665 (2004).
[39] J. L. F. Abascal and C. Vega, J. Chem. Phys. **123**, 234505 (2005).
[40] S. Piana, A. G. Donchev, P. Robustelli, and D. E. Shaw, J. Phys. Chem. B **119**, 5113 (2015).
[41] V. Cruces Chamorro, P. Jungwirth, and H. Martinez-Seara, J. Phys. Chem. Lett. **15**, 2922 (2024).
[42] R. Fuentes-Azcatl and J. Alejandre, J. Phys. Chem. B **118**, 1263 (2014).
[43] L.-P. Wang, T. J. Martinez, and V. S. Pande, J. Phys. Chem. Lett. **5**, 1885 (2014).
[44] S. Izadi, R. Anandakrishnan, and A. V. Onufriev, J. Phys. Chem. Lett. **5**, 3863 (2014).
[45] I. Leontyev and A. Stuchebrukhov, J. Chem. Phys. **130**, 085102 (2009).
[46] I. Leontyev and A. Stuchebrukhov, Phys. Chem. Chem. Phys. **13**, 2613 (2011).
[47] I. V. Leontyev and A. A. Stuchebrukhov, J. Chem. Theory Comput. **6**, 1498 (2010).
[48] J. K. Gregory, D. C. Clary, K. Liu, M. G. Brown, and R. J. Saykally, Science **275**, 814 (1997).
[49] Y. S. Badyal, M.-L. Saboungi, D. L. Price, S. D. Shastri, D. R. Haeffner, and A. K. Soper, J. Chem. Phys. **112**, 9206 (2000).
[50] M. Sharma, R. Resta, and R. Car, Phys. Rev. Lett. **98**, 247401 (2007).
[51] J. A. Morrone and R. Car, Phys. Rev. Lett. **101**, 017801 (2008).
[52] A. Krishnamoorthy, K. ichi Nomura, N. Baradwaj, K. Shimamura, P. Rajak, A. Mishra, S. Fukushima, F. Shimojo, R. Kalia, A. Nakano, and P. Vashishta, Phys. Rev. Lett. **126**, 216403 (2021).
[53] C. Vega, Mol. Phys. **113**, 1145 (2015).
[54] J. L. Aragones, L. G. MacDowell, and C. Vega, J. Phys. Chem. A **115**, 5745 (2011).
[55] S. Blazquez, J. L. F. Abascal, J. Lagerweij, P. Habibi, P. Dey, T. J. Vlugt, O. A. Moultos, and C. Vega, J. Chem. Theory Comput. **19**, 5380 (2023).
[56] M. Jorge and L. Lue, J. Chem. Phys. **150**, 084108 (2019).
[57] M. Jorge, M. C. Barrera, A. W. Milne, C. Ringrose, and D. J. Cole, J. Chem. Theory Comput. **19**, 1790 (2023).
[58] M. Neumann, Mol. Phys. **50**, 841 (1983).
[59] J. Kolafa and L. Viererblova, J. Chem. Theory Comput. **10**, 1468 (2014).
[60] P. Gallo, J. Bachler, L. E. Bove, R. Böhmer, G. Camisasca, L. E. Coronas, H. R. Corti, I. de Almeida Ribeiro, M. de Koning, G. Franzese *et al.*, Eur. Phys. J. E **44**, 143 (2021).
[61] J. L. F. Abascal and C. Vega, J. Chem. Phys. **134**, 186101 (2011).
[62] G. Pallares, M. A. Gonzalez, J. L. F. Abascal, C. Valeriani, and F. Caupin, Phys. Chem. Chem. Phys. **18**, 5896 (2016).
[63] C. Vega, J. L. F. Abascal, and I. Nezbeda, J. Chem. Phys. **125**, 034503 (2006).
[64] C. Vega and E. de Miguel, J. Chem. Phys. **126**, 154707 (2007).
[65] D. A. Case, H. M. Aktulga, K. Belfon, I. Ben-Shalom, S. R. Brozell, D. S. Cerutti, T. E. Cheatham III, V. W. D. Cruzeiro, T. A. Darden, R. E. Duke *et al.*, *Amber 2021*, University of California, San Francisco, CA, 2021.

[66]C. Tian, K. Kasavajhala, K. A. A. Belfon, L. Raguette, H. Huang, A. N. Migues, J. Bickel, Y. Wang, J. Pincay, Q. Wu, and C. Simmerling, J. Chem. Theory Comput. **16**, 528 (2020).
[67]S. Izadi and A. V. Onufriev, J. Chem. Phys. **145**, 074501 (2016).
[68]M. Perrone, R. Capelli, C. Empereur-Mot, A. Hassanali, and G. M. Pavan, J. Chem. Eng. Data **68**, 3228 (2023).
[69]H. Liu, Y. Wang, and J. M. Bowman, J. Chem. Phys. **142**, 194502 (2015).
[70]H. Liu, Y. Wang, and J. M. Bowman, J. Phys. Chem. B **120**, 1735 (2016).
[71]Z. Kann and J. Skinner, J. Chem. Phys. **141**, 104507 (2014).
[72]M. Kohagen, P. E. Mason, and P. Jungwirth, J. Phys. Chem. B **120**, 1454 (2015).
[73]E. Wernersson and P. Jungwirth, J. Chem. Theory Comput. **6**, 3233 (2010).
[74]Y. Yao, M. L. Berkowitz, and Y. Kanai, J. Chem. Phys. **143**, 241101 (2015).
[75]L. Perin and P. Gallo, J. Phys. Chem. B **127**, 4613 (2023).
[76]R. Robinson and R. Stokes, *Electrolyte Solutions*, 2nd ed. (Butterworths, London, 1959).
[77]G. M. Kontogeorgis, B. Maribo-Mogensen, and K. Thomsen, Fluid Phase Equilib. **462**, 130 (2018).
[78]B. Hess, H. Bekker, H. J. C. Berendsen, and J. G. E. M. Fraaije, J. Comput. Chem. **18**, 1463 (1997).
[79]M. Parrinello and A. Rahman, J. Appl. Phys. **52**, 7182 (1981).
[80]W. G. Hoover, Phys. Rev. A **31**, 1695 (1985).
[81]U. Essmann, L. Perera, M. L. Berkowitz, T. Darden, H. Lee, and L. G. Pedersen, J. Chem. Phys. **103**, 8577 (1995).
[82]V. Holten, C. E. Bertrand, M. A. Anisimov, and J. V. Sengers, J. Chem. Phys. **136**, 094507 (2012).
[83]S. Nosé and M. L. Klein, Mol. Phys. **50**, 1055 (1983).
[84]J. Rowlinson and B. Widom, *Molecular Theory of Capillarity* (Clarendon, Oxford, 1982).
[85]H. J. White, J. V. Sengers, D. B. Neumann, and J. C. Bellows, IAPWS Release on the Surface Tension of Ordinary Water Substance (1995).
[86]E. A. Guggenheim, J. Chem. Phys. **13**, 253 (1945).
[87]J. S. Rowlinson and F. L. Swinton, *Liquids and Liquid Mixtures* (Butterworths, London, 1982).
[88]M. A. González and J. L. F. Abascal, J. Chem. Phys. **132**, 096101 (2010).
[89]A. Ladd and L. Woodcock, Chem. Phys. Lett. **51**, 155 (1977).
[90]R. G. Fernandez, J. L. F. Abascal, and C. Vega, J. Chem. Phys. **124**, 144506 (2006).
[91]I. C. Yeh and G. Hummer, J. Phys. Chem. B **108**, 15873 (2004).
[92]E. W. Washburn and C. J. West, *International Critical Tables of Numerical Data, Physics, Chemistry and Technology* (National Academies, 1928), Vol. 3.
[93]J. Alejandre and G. A. Chapela, J. Chem. Phys. **132**, 014701 (2010).
[94]M. Chaplin https://water.lsbu.ac.uk/water/, 2006.
[95]H. White, J. Sengers, D. Neumann, and J. Bellows, Release on the surface tension of ordinary water substance (1995).
[96]J. Vrabec, G. K. Kedia, G. Fuchs, and H. Hasse, Mol. Phys. **104**, 1509 (2006).
[97]A. Trokhymchuk and J. Alejandre, J. Chem. Phys. **111**, 8510 (1999).
[98]J. Alejandre, D. J. Tildesley, and G. A. Chapela, J. Chem. Phys. **102**, 4574 (1995).
[99]G. J. gloor, G. Jackson, F. J. Blas, and E. de Miguel, J. Chem. Phys. **123**, 124703 (2005).
[100]G. A. Chapela, G. Saville, S. M. Thompson, and J. S. Rowlinson, Chem. Soc., Faraday Trans. **8**, 133 (1977).
[101]C. Tempra, O. H. S. Ollila, and M. Javanainen, J. Chem. Theory Comput. **18**, 1862 (2022).
[102]M. Lísal, W. R. Smith, and I. Nezbeda, Fluid Phase Equilib. **181**, 127–146 (2001).
[103]W. Wagner, A. Saul, and A. Pruß, J. Phys. Chem. Ref. Data **23**, 515 (1994).
[104]B. Guillot, J. Mol. Liq. **101**, 219 (2002).
[105]M. Jorge, J. R. B. Gomes, and A. W. Milne, J. Mol. Liq. **322**, 114550 (2021).
[106]P. Habibi, H. M. Polat, S. Blazquez, C. Vega, P. Dey, T. J. H. Vlugt, and O. A. Moultos, J. Phys. Chem. Lett. **15**, 4477 (2024).
[107]Y. Xiong, P. S. Shabane, and A. V. Onufriev, ACS Omega **5**, 25087 (2020).
[108]M. Conde, M. Rovere, and P. Gallo, J. Chem. Phys. **147**, 244506 (2017).
[109]M. D. Morse and S. A. Rice, J. Chem. Phys. **76**, 650 (1982).
[110]E. Whalley, J. Chem. Phys. **81**, 4087 (1984).
[111]J. Grabowska, S. Blazquez, E. Sanz, I. M. Zerón, J. Algaba, J. M. Míguez, F. J. Blas, and C. Vega, J. Phys. Chem. B **126**, 8553 (2022).
[112]S. Blazquez, C. Vega, and M. Conde, J. Mol. Liq. **383**, 122031 (2023).
[113]P. M. Piaggi, J. Weis, A. Z. Panagiotopoulos, P. G. Debenedetti, and R. Car, Proc. Natl. Acad. Sci. U. S. A. **119**, e2207294119 (2022).
[114]M. R. Walsh, C. A. Koh, E. D. Sloan, A. K. Sum, and D. T. Wu, Science **326**, 1095 (2009).
[115]L. Jensen, K. Thomsen, N. von Solms, S. Wierzchowski, M. R. Walsh, C. A. Koh, E. D. Sloan, D. T. Wu, and A. K. Sum, J. Phys. Chem. B **114**, 5775 (2010).
[116]V. Buch, P. Sandler, and J. Sadlej, J. Phys. Chem. B **102**, 8641 (1998).
[117]L. F. Sedano, S. Blazquez, E. G. Noya, C. Vega, and J. Troncoso, J. Chem. Phys. **156**, 154502 (2022).
[118]J. L. F. Abascal and C. Vega, J. Chem. Phys. **133**, 234502 (2010).
[119]R. J. Speedy and C. A. Angell, J. Chem. Phys. **65**, 851 (1976).
[120]P. H. Poole, F. Sciortino, U. Essmann, and H. E. Stanley, Nature **360**, 324 (1992).
[121]V. Babin, C. Leforestier, and F. Paesani, J. Chem. Theory Comput. **9**, 5395 (2013).
[122]V. Babin, G. R. Medders, and F. Paesani, J. Chem. Theory Comput. **10**, 1599 (2014).
[123]S. K. Reddy, S. C. Straight, P. Bajaj, C. Huy Pham, M. Riera, D. R. Moberg, M. A. Morales, C. Knight, A. W. Götz, and F. Paesani, J. Chem. Phys. **145**, 194504 (2016).
[124]P. Ren and J. W. Ponder, J. Phys. Chem. B **107**, 5933 (2003).
[125]P. Ren and J. W. Ponder, J. Phys. Chem. B **108**, 13427 (2004).
[126]D. Hare and C. Sorensen, J. Chem. Phys. **87**, 4840 (1987).
[127]V. Holten, J. V. Sengers, and M. A. Anisimov, J. Phys. Chem. Ref. Data **43**, 043101 (2014).
[128]T. Ando, J. Chem. Phys. **159**, 101102 (2023).
[129]C. Vega, M. M. Conde, C. McBride, J. L. F. Abascal, E. G. Noya, R. Ramirez, and L. M. Sese, J. Chem. Phys. **132**, 046101 (2010).
[130]S. L. Bore, P. M. Piaggi, R. Car, and F. Paesani, J. Chem. Phys. **157**, 054504 (2022).
[131]M. M. Conde, M. A. Gonzalez, J. L. F. Abascal, and C. Vega, J. Chem. Phys. **139**, 154505 (2013).
[132]A. K. Soper, Chem. Phys. **258**, 121 (2000).
[133]A. K. Soper, Int. Scholarly Res. Not. **1**, 279643 (2013).
[134]L. B. Skinner, C. Huang, D. Schlesinger, L. G. M. Pettersson, A. Nilsson, and C. J. Benmore, J. Chem. Phys. **138**, 074506 (2013).
[135]J. Cardona, M. Jorge, and L. Lue, Phys. Chem. Chem. Phys. **22**, 21741 (2020).
[136]B. Han, C. M. Isborn, and L. Shi, J. Phys. Chem. Lett. **14**, 3869 (2023).
[137]J. R. Reitz, F. J. Milford, and R. W. Christy, *Foundations of Electromagnetic Theory*, 4th ed. (Addison-Wesley, Reading, MA, 2000).
[138]D. A. McQuarrie, *Statistical Mechanics* (Harper and Row, New York, 1976).
[139]R. S. Berry, S. A. Rice, and J. Ross, *Physical Chemistry*, 2nd ed. (Oxford University Press, Oxford, 2000).
[140]I. N. Levine, *Physical Chemistry*, 1st ed. (McGraw-Hill, New York, 1978).
[141]W. R. Smith, I. Nezbeda, J. Kolafa, and F. Moučka, Fluid Phase Equilib. **466**, 19 (2018).
[142]S. H. Saravi and A. Z. Panagiotopoulos, J. Chem. Phys. **155**, 184501 (2021).
[143]Z. Mester and A. Z. Panagiotopoulos, J. Chem. Phys. **142**, 044507 (2015).
[144]A. Thum, A. Heuer, K. Shimizu, and J. N. Canongia Lopes, Phys. Chem. Chem. Phys. **22**, 525 (2020).
[145]C. M. Tenney, M. Massel, J. M. Mayes, M. Sen, J. F. Brennecke, and E. J. Maginn, J. Chem. Eng. Data **59**, 391 (2014).
[146]E. E. Fileti and V. V. Chaban, Chem. Phys. Lett. **616-617**, 205 (2014).
[147]V. V. Chaban, I. V. Voroshylova, and O. N. Kalugin, Phys. Chem. Chem. Phys. **13**, 7910 (2011).
[148]C. Schröder, Phys. Chem. Chem. Phys. **14**, 3089 (2012).
[149]I. M. Zeron, J. L. F. Abascal, and C. Vega, J. Chem. Phys. **151**, 134504 (2019).

[150]D. Biriukov, H.-W. Wang, N. Rampal, C. Tempra, P. Kula, J. C. Neuefeind, A. G. Stack, and M. Predota, J. Chem. Phys. **156**, 194505 (2022).
[151]E. Duboué-Dijon, P. E. Mason, H. E. Fischer, and P. Jungwirth, J. Phys. Chem. B **122**, 3296 (2017).
[152]M. Kohagen, P. E. Mason, and P. Jungwirth, J. Phys. Chem. B **118**, 7902 (2014).
[153]R. Fuentes-Azcatl, N. Mendoza, and J. Alejandre, Physica A **420**, 116 (2015).
[154]R. Fuentes-Azcatl and M. C. Barbosa, J. Phys. Chem. B **120**, 2460 (2016).
[155]J. L. F. Abascal, E. Sanz, R. G. Fernandez, and C. Vega, J. Chem. Phys. **122**, 234511 (2005).
[156]V. Molinero and E. B. Moore, J. Phys. Chem. B **113**, 4008 (2009).
[157]E. Duboue-Dijon, M. Javanainen, P. Delcroix, P. Jungwirth, and H. Martinez-Seara, J. Chem. Phys. **153**, 050901 (2020).
[158]L.-P. Wang, T. Head-Gordon, J. W. Ponder, P. Ren, J. D. Chodera, P. K. Eastman, T. J. Martinez, and V. S. Pande, J. Phys. Chem. B **117**, 9956 (2013).
[159]H. Jiang, O. A. Moultos, I. G. Economou, and A. Z. Panagiotopoulos, J. Phys. Chem. B **120**, 12358 (2016).
[160]X. Zhu, M. Riera, E. F. Bull-Vulpe, and F. Paesani, J. Chem. Theory Comput. **19**, 3551 (2023).
[161]Q. Yu, C. Qu, P. L. Houston, R. Conte, A. Nandi, and J. M. Bowman, J. Phys. Chem. Lett. **13**, 5068 (2022).
[162]P. Jedlovszky and R. Vallauri, Mol. Phys. **97**, 1157 (1999).
[163]T. Morawietz, A. Singraber, C. Dellago, and J. Behler, Proc. Natl. Acad. Sci. U. S. A. **113**, 8368 (2016).
[164]L. Zhang, J. Han, H. Wang, R. Car, and E. Weinan, Phys. Rev. Lett. **120**, 143001 (2018).
[165]A. K. Das, L. Urban, I. Leven, M. A. Aldossary, M. Head-Gordon, T. Head-Gordon, and T. Head-Gordon, J. Chem. Theory Comput. **15**, 5001 (2019).